Iranian Journal of Chemical Engineering
Vol. 3, No. 3 (Summer), 2006, IAChE

Research note

Asymptotic Analysis of Binary Gas Mixture Separation by Nanometric Tubular Ceramic Membranes: Cocurrent and Countercurrent Flow Patterns

*A. Razmjoo[1,2], A. A. Babaluo[*1,2,3], B. Bayati[1,2]*

1- Nanostructure Materials Research Center, Sahand University of Technology, P.O. Box 51335/1996, Tabriz, I. R. Iran.
2- Chemical Engineering Department, Sahand University of Technology, P.O. Box 51335/1996, Tabriz, I. R. Iran.
3- Research Center for Polymeric Materials, Sahand University of Technology, P.O. Box 51335/1996, Tabriz, I. R. Iran.

Abstract

Analytical gas-permeation models for predicting the separation process across membranes (exit compositions and area requirement) constitutes an important and necessary step in understanding the overall performance of membrane modules. But, the exact (numerical) solution methods suffer from the complexity of the solution. Therefore, solutions of nonlinear ordinary differential equations that govern the performance of the membrane modules for gas separations by approximate and asymptotic methods are useful in the design and comparison of processes. In this work, the asymptotic methods were applied for predicting the performance of nanometric tubular ceramic membranes in the separation of binary gas mixtures with cocurrent and countercurrent flow patterns. Also, the exact (numerical) solutions of the governing equations using the fourth order Rung-Kutta technique were proposed. The comparison of the results showed a good agreement between the exact solution and asymptotic analysis methods over the whole range of selectivities ($1 \le \alpha \le \infty$). Because, the asymptotic curves into the former ($\alpha \to 1$) and latter ($\alpha \to \infty$) boundaries had a suitable overlap with each other to cover the whole range of selectivities. The accuracy of this method was verified by a comparison of the predicted results with different literature experimental data and mathematical models. This result suggests the use of the asymptotic analysis method to provide excellent shortcut, preliminary design information.

Keywords: *Nanometric Membrane, Binary Mixture, Gas Separation, Asymptotic Analysis*

Introduction

Membranes have gained an important place in chemical technology and are used in a broad range of applications. The key property that is exploited is the ability of membrane to control the permeation rate of a chemical species through the membrane. In separation application, the goal is to allow one component of a mixture to permeate the membrane freely, while hindering permeation of other components [1].

* - Corresponding author: E-mail: a.babaluo@sut.ac.ir

The separation of gas mixture by membranes in nanometric scales has emerged from being a laboratory curiosity to becoming a rapidly growing and commercially viable alternative to traditional methods of gas separation within the last two decades [2]. The nonlinear ordinary differential equations that govern the performance of the membrane modules for gas separations are well known. These equations have been solved by many investigators [3-9]. Shindo et al. [5] developed approximate calculation methods for multicomponent separations in five flow patterns: one-side mixing, complete mixing, cross flow, countercurrent and cocurrent flow. Krovvidi et al. [8] tried solving the governing differential equations directly as a two-point boundary value problem using shooting techniques. Coker et al. [9] used a staged approach (100–1,000 stages) to convert the pertinent differential equations to a set of coupled, non-linear difference equations. This corresponds to a first order finite difference methodology, with an iterative solution of the derived tridiagonal matrices. For highly simplified cases such as perfectly mixed residue and feed, analytical solutions are available [10]. Kaldis et al. used the orthogonal collocation technique to solve the mathematical model that describes the binary and multi-component gas mixture separation in hollow fiber asymmetric membranes [11,18]. In each of the numerical solutions described above the numerical methods suffer from the complexity of the solution. Solutions for complex cases can be obtained by series approximations or asymptotic analysis of the underlying differential equations governing mass transfer and pressure distribution in the module [4,7,8]. Search for approximate solutions started with Boucif and co-workers [4] by expressing the feed and permeate composition as a series function of a dimensionless membrane area. Basaran and Auvil [7] approached the problem of binary gas separation by the cross-flow pattern with an asymptotic analysis, choosing the extremes in selectivity ($\alpha \to 1$ and $\alpha \to \infty$) as the asymptotic regimes. Smith et al. [12] used asymptotic analysis for modeling the completely mixed flow pattern. What has been lacking in the literature is an analysis by asymptotic methods that provide valuable insight into the performance of the membrane module in certain limiting regimes of their operations. Therefore, the use of asymptotic methods in the preliminary design of the gas permeator is necessary because of savings in time and resources.

In this research, the performance of the nanometric membranes in the gas separation processes was investigated and the behavior of the permeator under extreme operating conditions was predicted for cocurrent and countercurrent flow patterns by using the asymptotic methods. Also the exact (numerical) solution of the governing differential equations was presented in this paper. Finally, the results of the asymptotic methods were compared with the exact solution. The ceramic nanocomposite membranes manufactured in our previous study, fall into the former boundary ($\alpha \to 1$). By way of example, hydrogen to methane selectivity is about 2.8 in these membranes [13]. Most modified membranes in the future our works can be seen to fall in the latter class ($\alpha \to \infty$).

Theory

Asymptotic Methods

As mentioned before, the aim of this paper is to gain a good understanding of membrane performance for binary mixtures without resorting to extensive numerical calculations. In fact, the formulas obtained are simple enough in form to make them suitable for rapidly estimating membrane performance. The asymptotic expressions for the mole fractions (as functions of area) can be used for rapidly estimating the membrane area and the membrane cost required to affect a

desired separation. Basaran and Auvil [2] have presented this research for the first time in 1988. Their equations that govern the performance of membrane modules have been solved in their paper by asymptotic methods for the case of a binary gas mixture in a cross-flow module. They introduce a relation for the total molar flow rate and mole fraction of fast permeating gas as a function of the dimensionless membrane area. Cocurrent and countercurrent flow patterns are the most advantageous and practical among the other flow patterns and there is not any asymptotic analysis for these two kinds of flow patterns in the literature.

There are four steps for estimating membrane performance in asymptotic analysis (see Fig.1). The limits as $\alpha \to 1$ and $\alpha \to \infty$, where α is the selectivity of the fast-permeating gas with respect to the slow-permeating gas, are identified as the two asymptotic regimes. Membranes that have a selectivity of order 1 or much greater than 1 abound in practice. These estimations can be used before simulating any models of permeators in order to have good limitation.

Governing Equation

The present models are developed based on the equations formulated by Krovvidi et al [8], based on the following assumptions:

- The tubular ceramic-composite membranes consist of a very thin nanometric top-layer based on the alumina porous support system.
- The feed is a binary gas mixture and there is no purge on the permeate side
- The permeability coefficient of each component is that of the pure component and is unaffected by the presence of other components and by pressure
- Negligible pressure drop is experienced by feed and permeate streams
- Feed and permeate streams are in plug flow.

The development of the asymptotic methods in cocurrent and countercurrent situations is presented below.

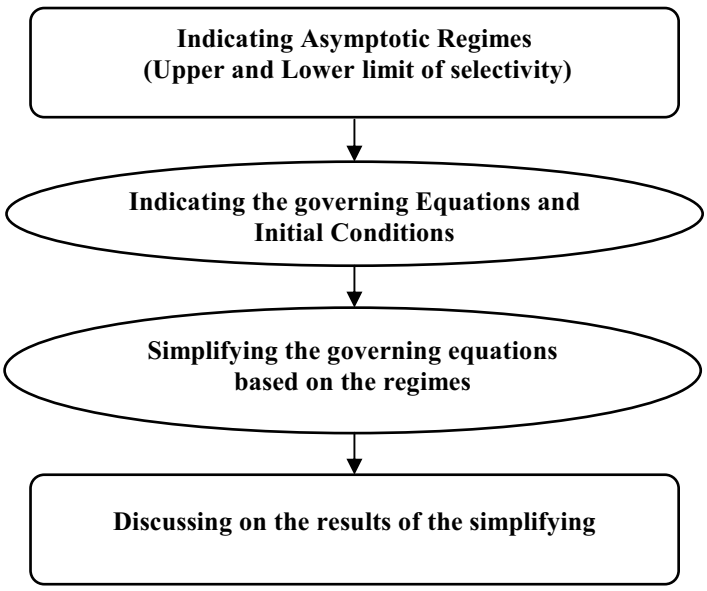

Figure 1. Schematic diagram for estimating the membrane performance by asymptotic method

I. Cocurrent flow pattern

Fig. 2a is a schematic diagram of a cocurrent permeator. The material balance and transport equations are written with respect to the feed entry point. Eqns (1)-(4) is the overall material and component balances for this case in dimensionless form and the differential equations for component molar flow rates along the permeator for the feed and permeate sides.

$$L^* + V^* = 1 \tag{1}$$

$$L^* x + V^* y = x_f \tag{2}$$

$$-\frac{d(L^* x)}{d(R^f)} = \frac{d(V^*.y)}{d(R^f)} = \alpha(x - \gamma y) \tag{3}$$

$$-\frac{d(L^*)}{d(R^f)} = \frac{d(V^*)}{d(R^f)} = \alpha(x - \gamma y) + [(1 - x) - \gamma(1 - y)] \tag{4}$$

Combining eqns (1)-(4) and simplifying, the following equations for the variations in compositions along the permeator are obtained:

$$\frac{dx}{dR^f} = \frac{(x - y)\{\alpha(1 - x)(x - \gamma y) - x[1 - x - \gamma(1 - y)]\}}{(y - x_f)} \tag{5}$$

and

$$\frac{dy}{dR^f} = \frac{(y - x)\{\alpha(1 - y)(x - \gamma y) - y[1 - x - \gamma(1 - y)]\}}{(x_f - x)} \tag{6}$$

The initial conditions are:

$$L^* = 1; \quad V^* = 0; \quad x = x_f; \quad y = y_f; \quad at \ \ R^f = 0 \tag{7}$$

II . Countercurrent flow pattern

In the countercurrent flow pattern (Fig. 2b), the contacting streams flow in opposite directions. Material balance and transport equations are rewritten for this case with reference to the residue end for easing of computation. The equations resulting from this material balance are the same as eqns (1)-(4), the only difference being that superscripts and subscripts f and w should be interchanged.

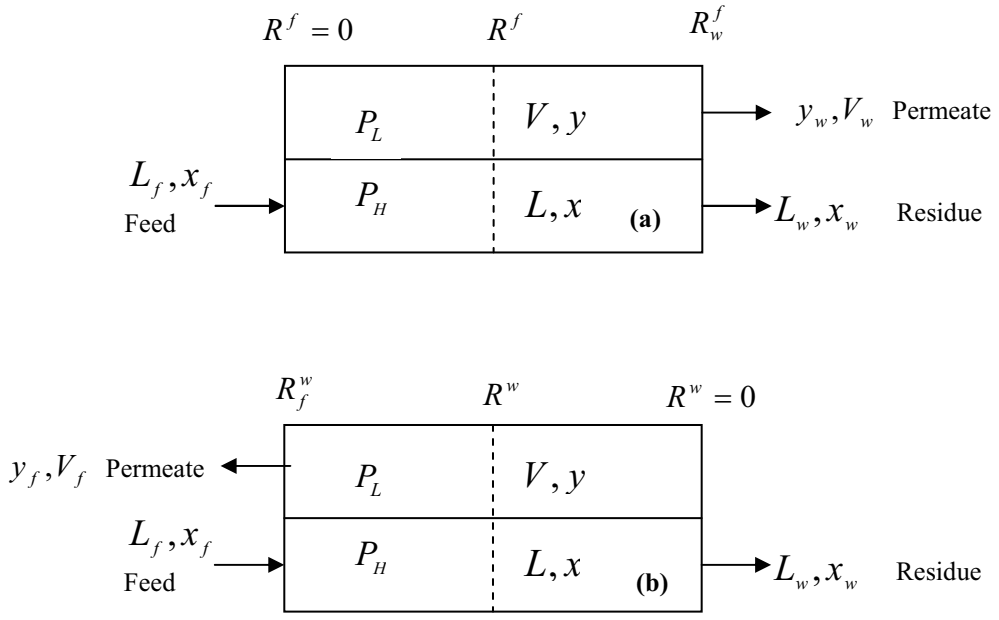

Figure 2. Schematic diagram of a **(a)** cocurrent and **(b)** countercurrent binary gas permeator

The dimensionless membrane area R^W resulting from interchange is defined by:

$$R^w = \frac{P_H A K_2}{L_w} \tag{8}$$

The actual membrane area, *A,* is measured from the residue end in the countercurrent case and the relationship between R^w and R^f, using equation (1) and (2), is given by

$$R^f = \frac{(x_f - y_f)}{(x_w - y_f)}\left(R_f^w - R^w\right) \tag{9}$$

so

$$dR^f = -\frac{(x_f - y_f)}{(x_w - y_f)} dR^w \tag{10}$$

Eqns (5) and (6) are modified by using of eq. (10)

$$\frac{dx}{dR^w} = -\frac{(x_f - y_f)}{(x_w - y_f)} \cdot \frac{(x-y)\{\alpha(1-x)(x-\gamma y) - x[1-x-\gamma(1-y)]\}}{(y - x_f)} \tag{11}$$

and

$$\frac{dy}{dR^w} = -\frac{(x_f - y_f)}{(x_w - y_f)} \cdot \frac{(y-x)\{\alpha(1-y)(x-\gamma y) - y[1-x-\gamma(1-y)]\}}{(x_f - x)} \tag{12}$$

The initial conditions are:

$$L^*(L/L_w) = 1; \quad V^* = 0; \quad x = x_w; \quad y = y_w; \quad at \;\; R^w = 0 \tag{13}$$

For a binary mixture, the mole fraction y_f at $R^f = 0$ in cocurrent flow pattern and y_w at $R^w = 0$ in countercurrent flow pattern can be calculated by the following expressions [5]:

$$\frac{\alpha x_i}{\gamma\{\alpha - 1\} - (1 - x_i)/(1 - y_i)} + (1 - y_i) = 1 \qquad i = f, w \tag{14}$$

Rearranging equation 14 and solving the quadratic formula yields:

$$y_i = \frac{1 + (\alpha - 1)(\gamma + x_i) - \left\{[1 + (\alpha - 1)(\gamma + x_i)]^2 - 4\gamma\alpha(\alpha - 1)x_i\right\}^{1/2}}{2\gamma(\alpha - 1)} \qquad i = f, w \tag{15}$$

Computations are performed starting from the residue end in terms of the R^w in the countercurrent situation as mentioned above. However, results are presented in terms of R^f for comparison purposes.

Governing Equations with Asymptotic Regimes

I. Lower Limit ($\alpha \to 1$)

When the permeabilities of the two gases are equal ($\alpha = 1$):

$$y = x = x_{in} \tag{16}$$

By using equation 4, L* can be calculated from the below equation:

$$L^* = 1 + (\gamma - 1)R^f \tag{17}$$

In case of nearly equal permeabilities ($\alpha \to 1$), solution of eqns (4)-(6) are sought by expanding the unknown x, y and L^* in powers of the small parameter ($\alpha - 1$), where the zero order solution is $y_0 = x_0 = x_f$ and $L_0^* = 1 + (\gamma - 1)R^f$, and the first order solution is $y_1 = x_1 = -(1 - x_f)x_f(1 - \gamma)R_f$ and

$L_1^* = -x_f(\gamma - 1)R^f$. The expansion is truncated to the first order of $(\alpha - 1)$ term as follows:

$$x = x_0 + x_1(\alpha - 1) \tag{18}$$

$$y = y_0 + y_1(\alpha - 1) \tag{19}$$

$$L^* = L_0^* + L_1^*(\alpha - 1) \tag{20}$$

Detailed deviations of eqns (18)-(20) are presented in appendix A

II. Upper Limit ($\alpha \to \infty$)

When the permeability of the fast gas is infinitely large compared to that of the slow permeable gas, the membrane is infinitely selective, $\alpha \to \infty$ and mole fraction of the fast permeating component on the permeate side is equal to one ($y = 1$), because there is not any slower component on the permeate side. Eq.(5) reduces to:

$$\frac{dx}{dR^f} = \frac{(1-x)^2\{\alpha(x-\gamma)-x\}}{(x_f - 1)} \tag{21}$$

L* is calculated from eqns (1) and (2):

$$L^* = {(x_f - y)}\Big/{(x - y)} \tag{22}$$

In the case of very different permeabilities, y =1, eq. (22) can be written as follows:

$$L^* = {(x_f - 1)}\Big/{(x - 1)} \tag{23}$$

For countercurrent operation the modification is similar to the cocurrent operation. Eqns (18) and (21) gives the total dimensionless membrane area (R_w^f) required to achieve a desired separation, from a given feed composition *(x_f)* to the desired residue composition *(x_w)*. For determining the residue composition (x_w) for a given membrane area (R_w^f) these equations must be solved by a backward procedure.

Result and Discussion

Result of the asymptotic method compared with the exact solution, are presented below for cocurrent and countercurrent flow patterns. For exact solution, eqns (5)-(6) and (11)-(12) are solved using the fourth order Rung-Kutta technique.

In Fig. 3, the predictions of the asymptotic analysis for $\alpha \to 1$ are compared to an exact solution in which $x_f = 0.1,\ \gamma = 0.1$ and $\alpha = 2$ or $\alpha = 1.2$. Fig. 3 shows that the agreement between the exact and approximate solutions is good when selectivity tend to unit. Also, countercurrent flow gives a more satisfactory agreement than cocurrent when selectivity tends to unite. The deviation for cocurrent from asymptotic is slightly greater than countercurrent in $\alpha = 1.2$. In case of nearly equal permeabilities the asymptotic method for countercurrent operation is more suitable than cocurrent and provides a convenient method for short-cut design estimation of membrane module performance.

In Fig. 4a the predictions of the asymptotic analysis for $\alpha \to \infty$ are compared to those of numerically solving eqns (5)-(6) for situations in which $x_f = 0.1, \gamma = 0.1$ and $\alpha = 1000$. The flow pattern is cocurrent and equations are integrated until $x_w = 0.105$.

Fig. 4a shows that the agreement between the exact and approximate solutions is excellent when selectivity tends to the infinite. Mole fraction on the permeate side y, also shows very good agreement as the length of the whole module is traversed, while the results of Basaran and Auvil [7] shows that the permeate side mole fraction y, varies by 7% from its initial value of one as the length of the whole module is traversed (see Fig. 4b).

Fig. 5 shows the *x, y* and *L** versus R^f for cocurrent, countercurrent and asymptotic for the same conditions of Fig. 4. As can be seen,

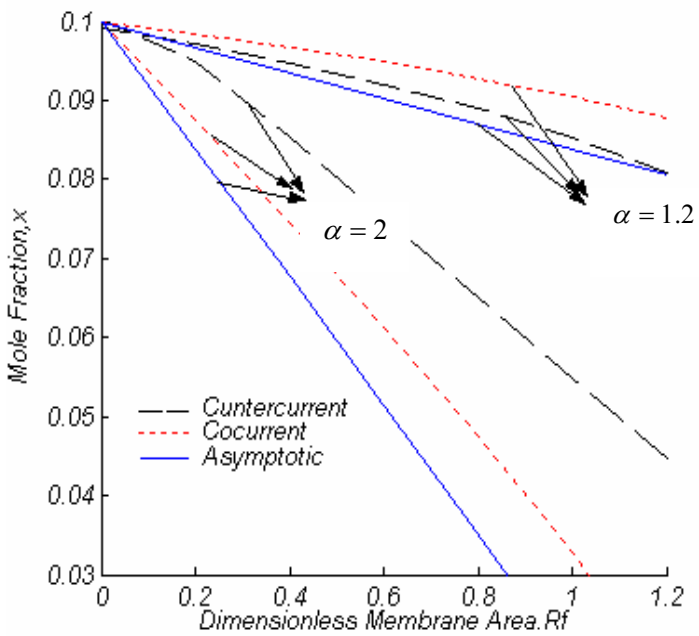

Figure 3. x-R^f profile for cocurrent and countercurrent flow patterns ($x_f = 0.1, \gamma = 0.1$)

the x, y and L^* versus R^f behavior predicted by the asymptotic method compares well with the pattern obtained by an exact solution of cocurrent and countercurrent. This justified the assumption involved in the development of the asymptotic governing equations. The asymptotic prediction of y, for cocurrent flow pattern gets better than countercurrent with increasing R^f due to describing the results of countercurrent in terms of R^f for comparison purposes. As shown in Fig. 5, the mole fraction, y for cocurrent flow pattern reduces by 0.4% from its initial value of one as the length of the whole module is traversed and for cross flow from Basaran and Auvil [7] is 7%. But, separation in the countercurrent flow pattern shows the mole fraction, y increases by 2% from its initial value at $R^w=0$ as the length of the whole module is traversed. For conditions of Fig. 4 the outlet permeate composition (y_f) for countercurrent flow is 0.994 and the outlet permeate composition (y_w) for cocurrent flow is 0.992. This difference for large membrane surfaces can be more significant. Therefore, countercurrent flow shows the better performance in the present calculation. Fig. 5 also shows that the asymptote's curve is between the exact solution of cocurrent and countercurrent curves. This validates the use of asymptotic analysis for rapid estimation of membrane performance before choosing any kind of exact flow pattern.

Fig. 6 is the asymptotic total membrane area as a function of the mole fraction of the fast gas at module exit. In the large selectivities, little membrane area is required if $x_w \geq \gamma$. However, the total membrane area becomes very large if $x_w << \gamma$. For example, at $\gamma = 0.3$, the required total membrane area when $x_w = 0.24$ is about four times greater than $x_w = 0.25$. Its physical meaning is that a membrane module in gas separation processes has the capacity to separate components till a critical concentration (x_{wc}) and by further increasing of the membrane

module area, x_w this capacity does not decrease significantly. Also, by decreasing γ (i.e. increasing pressure driving force), the critical concentration (x_{wc}) decreases (as shown in Fig.6). This is the primary reason for applying multistage systems in gas separation processes.

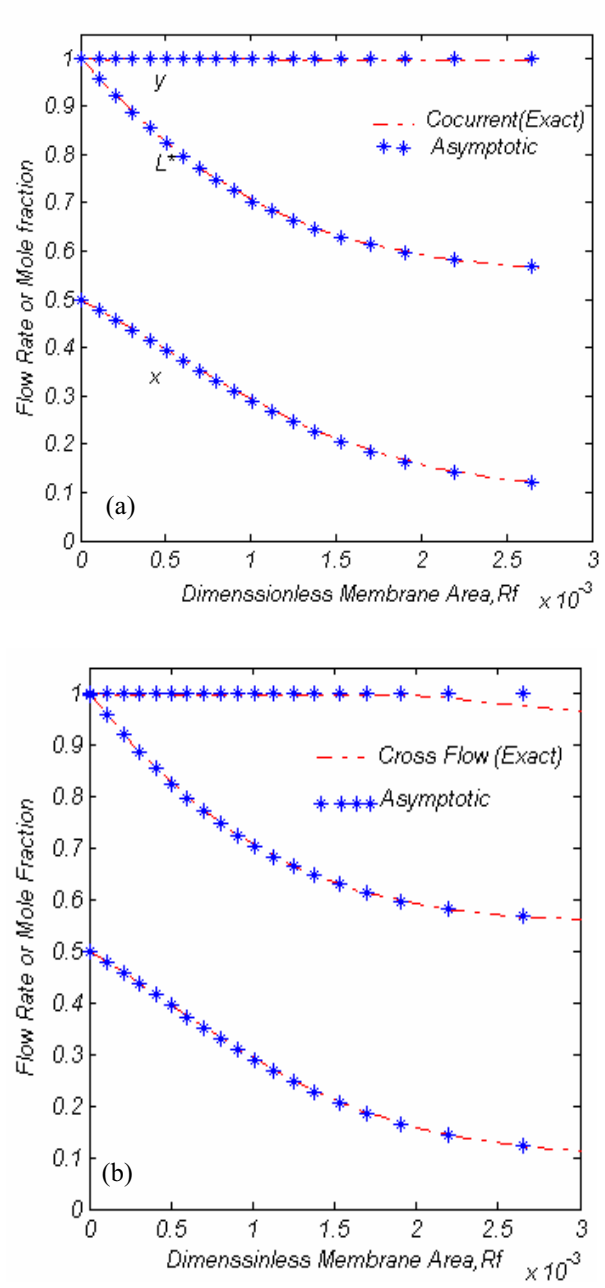

Figure 4. *x, y* and L* versus R^f for (a)Cocurrent (b) Cross flow [2]
($x_f = 0.5, \gamma = 0.1$ and $\alpha = 1000$)

Fig.7 shows how the dimensionless membrane area varies with the selectivity. The membrane area shown is required to reduce the mole fraction of the fast gas in the feed from 0.4 to 0.2. In Fig. 7, the asymptotic results (for $\alpha \to 1$ and $\alpha \to \infty$) and the numerical results (for cocurrent and countercurrent flow patterns) are in excellent agreement over the whole range of selectivity. Under the condition of Fig. 7, the asymptotic curve when $\alpha \to 1$, is in agreement by cocurrent and countercurrent curves until $\alpha = 10$ and $\alpha = 12$, respectively. Also, the asymptotic curve when $\alpha \to \infty$, is in agreement by cocurrent and countercurrent curves for selectivities more than 10 and 12, respectively. In this case, the numerical calculation and the $\alpha \to \infty$ asymptotic show that the membrane area required to affect a separation, approaches zero when the selectivity approaches infinity. This is physically plausible because the separation occurs inside a thin-boundary layer at the entrance to the module. In Fig.7, the asymptotic and the numerical results are in excellent agreement over the whole range of selectivities ($1 \le \alpha \le \infty$). Therefore, it can be concluded that the obtained simple formulas in *Asymptotic Analysis method* are suitable for rapidly estimating the membrane performance in the whole range of selectivities.

Verification of the Asymptotic Method

Sridhar et al.[14] used four stages of a cascade configuration which were required for obtaining a 99% permeate product stream. Their model was used for the separation of propylene and propane by an ethyl cellulose membrane. In Fig. 8, their model results are compared with the ones computed by the asymptotic method. For this computation, the dimensionless membrane area and operating conditions of Sridhar et al. have been used as a function of the stage cut; (V_w/L_f) and (V_f/L_f) for concurrent and countercurrent flow patterns, respectively. The overall

agreement is good and the maximum discrepancies between the Asymptotic solutions and Sridhar et al's predictions are less than 5%.

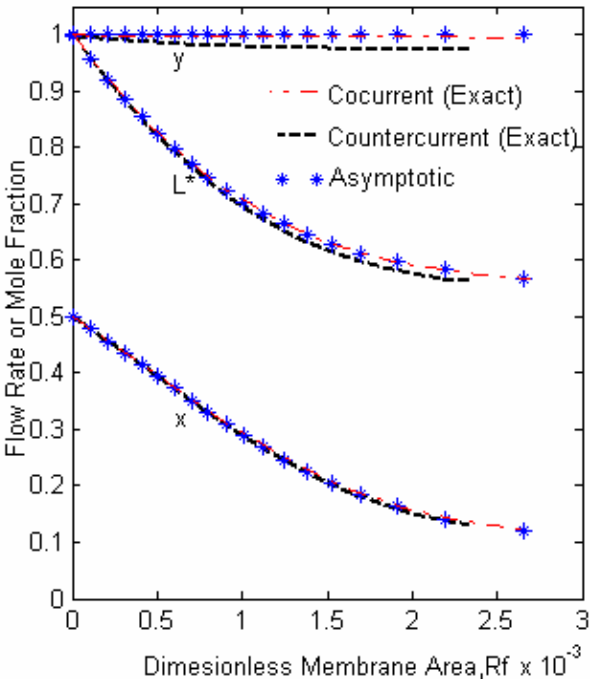

Figure 5. x, y and L^* versus R^f for Cocurrent and Countercurrent flow patterns ($x_f = 0.5, \gamma = 0.1$ and $\alpha = 1000$)

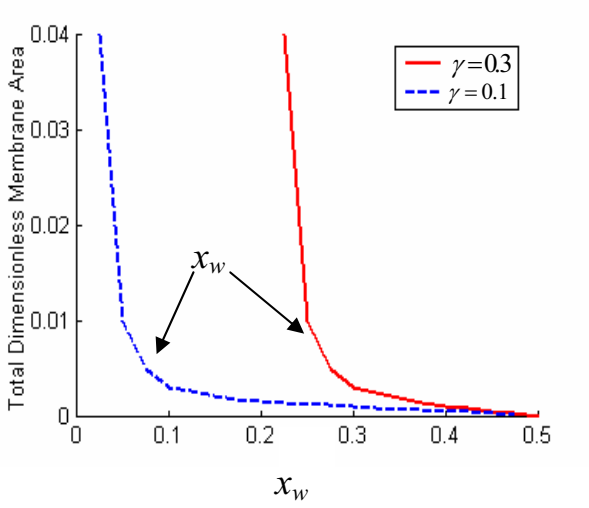

Figure 6. x_w versus total dimensionless area for different γ values ($x_f = 0.5, \alpha = 1000$)

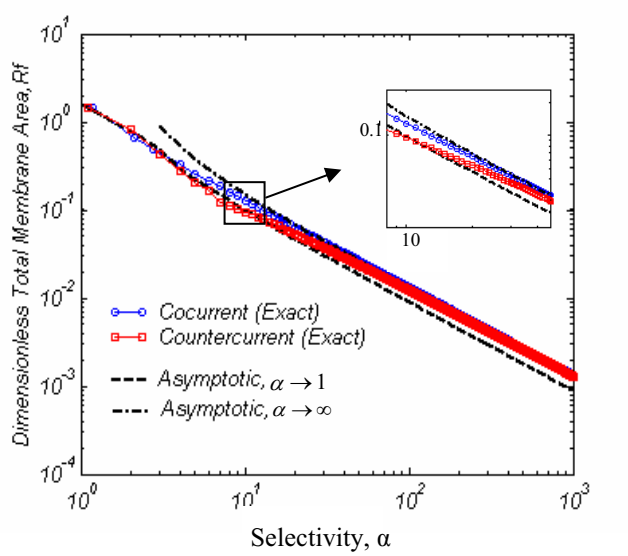

Figure 7. Total dimensionless area as a function of selectivity for cocurrent and countercurrent flow pattern ($x_f = 0.4, \gamma = 0.1$ and $x_w = 0.2$)

Verification of the Asymptotic Method

Sridhar et al.[14] used four stages of a cascade configuration which were required for obtaining a 99% permeate product stream. Their model used for the separation of propylene and propane by ethyl cellulose membrane. In Fig. 8, their model results are compared with the ones computed by the asymptotic method. For this computation, the dimensionless membrane area and operating conditions of Sridhar et al. have been used as a function of the stage cut; (V_w/L_f) and (V_f/L_f) for concurrent and countercurrent flow patterns, respectively. The overall agreement is good and the maximum discrepancies between the Asymptotic solutions and Sridhar et al's predictions are less than 5%.

Figs (9) shows the typical feed and permeate concentration profile for cocurrent and countercurrent flow patterns as obtained with the use of the proposed solution technique (asymptotic) and compared with the ones obtained with Pan's solution technique [15] under the same operating conditions. Both methods give essentially identical results, but the proposed asymptotic method requires less

effort in computing because it solves simplified analytical expressions.

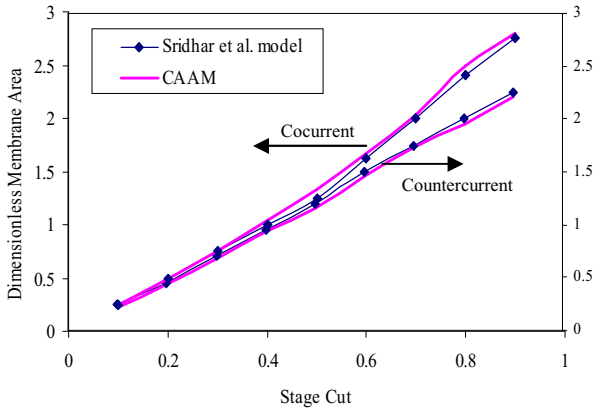

Figure 8. Comparison between Sridhar et al. ([14]) model and asymptotic method for variation of dimensionless membrane area with stage cut in cocurrent & countercurrent flow patterns

Excellent agreements are also observed in Fig.10, where the asymptotic method was compared with the model and experimental results of Conesa et al [16]. They used a nanometric tubular ceramic membrane (pore radiuses 25-41 nm) with two successive layers of alumina for decreasing pore size and a sol-gel top layer. They tried to predict the optimal performance conditions and the total yield of a membrane if the permeability of the gases to be separated is known as a function of the mean pressure. As can be seen in Fig. 10, the agreements between the asymptotic method and the Conesa et al.'s experimental data is better than their model. It may be attributed to the consideration of the feed and permeate streams as plug flows in this study, while Conesa et al. assumed that the composition of the gas mixtures on the high and low pressure sides was the same as that of the residue and permeate streams, respectively.

Giglia et al. [17] used three permeators in series and they reported the concentrations measured at the end of each permeator. In Fig. 11a, those results were compared with the ones computed by the asymptotic method. For this computation, the membrane dimensions and operating conditions of Giglia et al. were used. The present model overpredicts the y values, because, by neglecting the pressure drop in the permeate side, the maximum pressure driving force is assumed in the whole length of the membrane module,

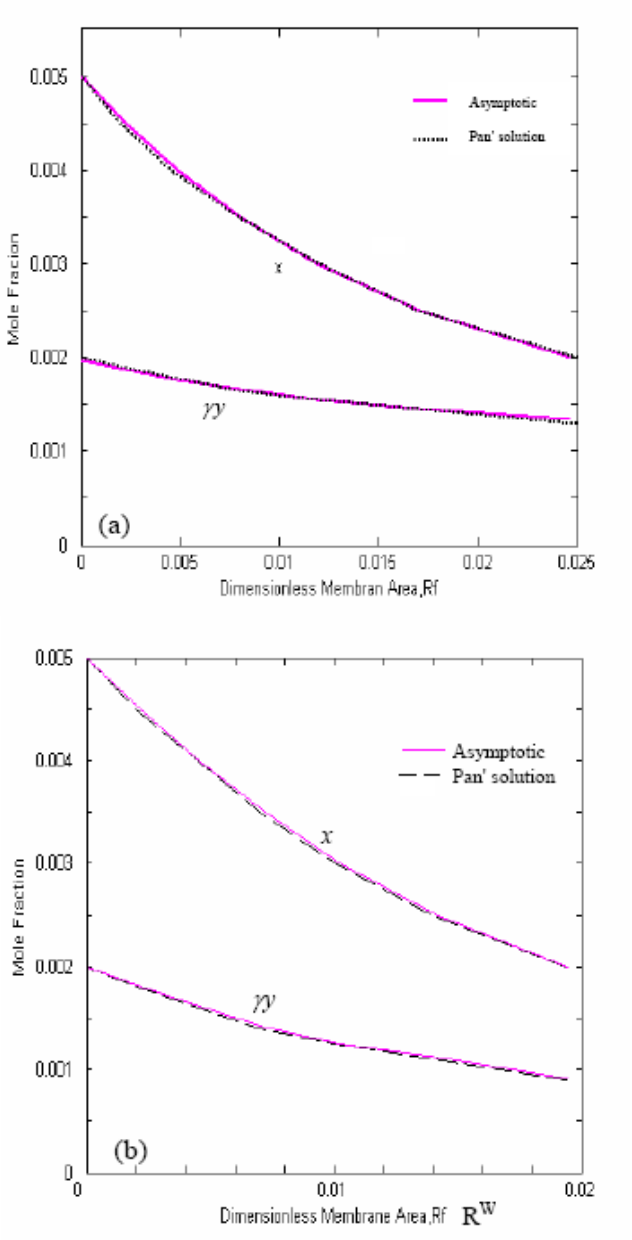

Figure 9. Comparison between Pan's [15] solution and Asymptotic method for feed and permeate concentration profile for (a) cocurrent (b) countercurrent flow patterns

whereas it can be obtained in the end of the module (permeate flow end) when the permeate pressure drop is considered. But, the discrepancies between the asymptotic method predictions and Giglia et al.'s experimental data are about less than 4%. Therefore, the overall agreement is good and this method assumption has little effect on the prediction results. The accuracy of this claim can be verified by comparison with literature data. In Fig. 11b, where the present model and Giglia et al.'s experimental data were compared with results of Kaldis et al.'s model [18]. In spite of considering the drop in pressure by the permeate stream in the Kaldis et al. model, similar differences in the computed permeate concentration are also observed.

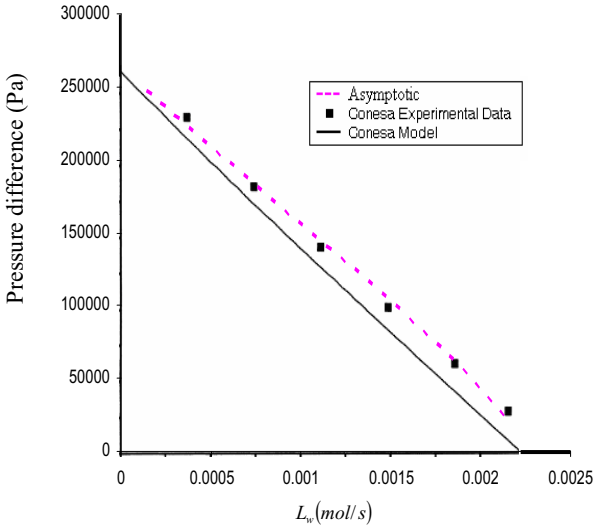

Figure 10. Comparison between Conesa et al. [16] and asymptotic method for pressure difference versus residue flow.

Conclusion

The asymptotic analysis method was used to predict the performance of the nanometric tubular ceramic membranes with cocurrent and countercurrent flow patterns, in this study. Also, the governing nonlinear ordinary differential equations were solved using the fourth order Rung-Kutta technique. Finally the Asymptotic method was verified by different literature experimental data and rigorous models.

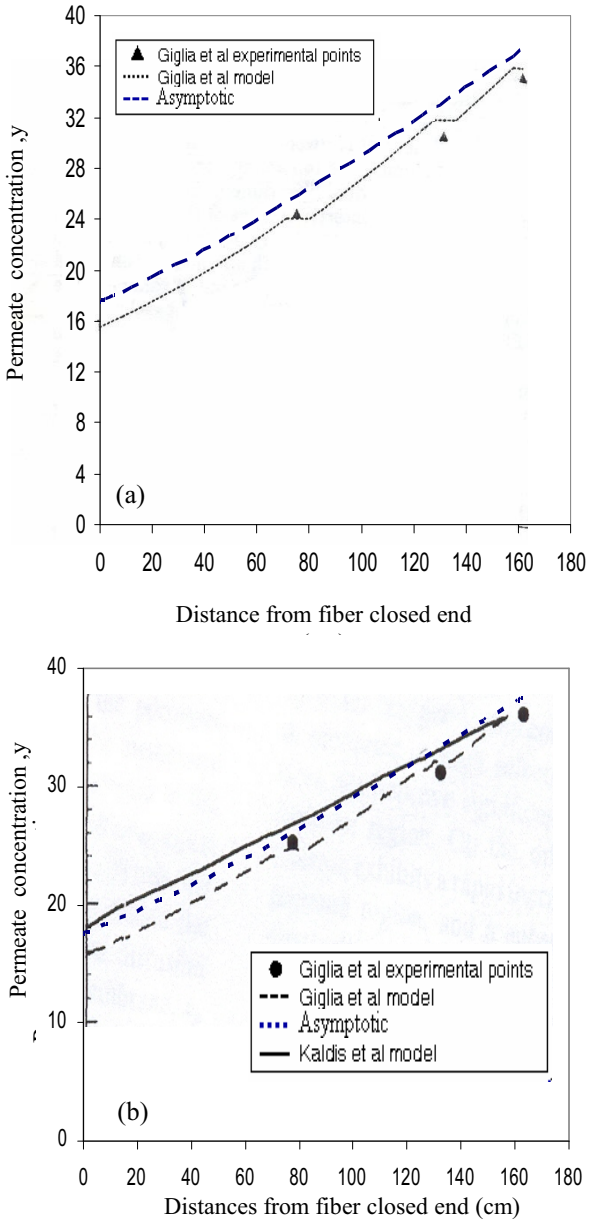

Figure 11. Comparison between Giglia et al. [17] and asymptotic method and Kaldis et al [18] model for permeate concentration profiles along an asymmetric hollow fiber membrane operating in countercurrent.

General conclusions obtained from the comparison of the asymptotic analysis and exact solution results can be presented as follows:

- At the former boundary ($\alpha \to 1$), the agreement between the exact and approximate solutions is good when selectivity tends to unite. Also, countercurrent flow gives more satisfactory agreement than cocurrent when selectivity tends to unite.
- At the latter class ($\alpha \to \infty$), the agreement between the exact and approximate solutions is excellent when selectivity tends to the infinite.
- Countercurrent flow pattern showed better performance in the membrane modules for gas separation processes than the cocurrent flow pattern, especially in the large surface area of membrane modules.
- In the large selectivities, the total membrane area becomes very large if $x_w << \gamma$. Therefore, the operating condition must be limited to $x_w \geq \gamma$.
- The asymptotic results (for $\alpha \to 1$ and $\alpha \to \infty$) and the numerical results (for cocurrent and countercurrent flow patterns) are in excellent agreement over the whole range of selectivity.
- The asymptotic curves into the former ($\alpha \to 1$) and latter ($\alpha \to \infty$) boundaries overlap each other sufficiently to cover the whole range of selectivities.

Therefore, the results confirm the use of asymptotic analysis for rapid estimation of membrane performance before choosing any kind of the exact flow pattern.

Nomenclature

A	Membrane area (m^2)
d	Effective membrane thickness (m)
L	Molar flow rate of the feed stream (mol/(m^2-sec))
L^*	Dimensionless feed–side flow rate= L/L_f in cocurrent, L/L_w in countercurrent
P_H	Feed side pressure (Pa)
P_L	Permeate side pressure (Pa)
K	Permeability coefficient ([m^3 (STP)-m]/(m^2-sec-Pa))
R^f	$\frac{P_H AK}{L_f}$; Dimensionless membrane area measured from feed inlet
R^w	$\frac{P_H AK}{L_w}$; Dimensionless membrane area measured from residue end
R_w^f	Total dimensionless membrane area defined with respect to L_f
R_f^w	Total dimensionless membrane area defined with respect to L_w
V	Molar flow rate of the permeate stream (mol/(m^2-sec))
V^*	Dimensionless permeate–side flow rate= V/L_f in cocurrent, V/L_w in countercurrent
x	Mole fraction of the fast permeating component on the feed side
y	Mole fraction of the fast permeating component on the permeate side
Subscripts	
f	Feed inlet
w	Residue end
Greek symbols	
α	Selectivity of the membrane for the more permeable component, K_1/K_2

γ	Ratio of the permeate-side pressure to feed side pressure ($\frac{P_L}{P_H}$)

Acknowledgements
The Authors wish to thank Sahand University of Technology (SUT) and Tabriz refinery for the financial support of this work. Also, we would like to thank our co-workers and technical staff in the department of chemical engineering, research center for polymeric materials and nanostructure materials research center of SUT for their help during various stages of this work.

Reference

1. Baker, R. W., Membrane Technology and Applications, Jone Wiely and Sons, Ltd ISBN: 0-470-85445-6, (2004).
2. Nunes, S. P. and Peinemann.V. K., Membrane Technology in Chemical Industry, Wiely-Vch, ISBN: 3-527-28485-0, (2001).
3. Hwang, S.T. and Kammermeyer, K., Membranes in Separations, Wiley-Interscience, New York, NY, (1975).
4. Boucif, N., Majumdar, S. and Sirkar, KK., Series solution for a gas permeator with countercurrent and cocurrent flow, Ind. Eng. Chem. Fundam., **23,** 470(1984).
5. Shindo, Y., Hakuta, T. and Yohitome, H., Calculation Methods for Multicomponent Gas Separation by Permeation, Separation Science and Technology, **20**(5 & 6), 445-459 (1985).
6. Pan, C. Y., Gas Separation by High-Flux**,** Asymmetric Hollow-Fiber Membrane, AIChE Journal, **32** (12), 2020-2070 (1986).
7. Basaran , O. A., Auvil, S. R., Asymptotic Analysis of Gas Separation by a Membrane Module, AIChE October, **34** (10), 1726-1731 (1988).
8. Krovvidi, K. R., Kovvali, A.S., Vemury, S. and Kh, A.A., Approximate solutions for gas permeator separating binary mixtures, Journal of Membrane Sci., **66,** 103-118 (1992).
9. Coker, D. T., Freeman, T. B. D. and Fleming, G. K.**,** Modeling multi-component gas separation using hollow-fiber membrane contactors, AIChE Journal, **44** (6), 1289-1302 (1998).
10. Smith, S. W., Freeman, B. D., Hall, C. K. and Rautenbach, R., Analytical Gas Permeation Models for Binary Gas Mixture Separation Using Membrane Modules, Journal of Membrane Science, **118**, 289 (1996).
11. Kaldis, S. P., Kapantaidakis, G. C. and Sakellaropoulos, G. P., Simulation of multicomponent gas separation in a hollow fiber membrane by orthogonal collocation-hydrogen recovery from refinery gases, Journal of Membrane Science, **173,** 61–71 (2000).
12. Smith, S.W., Hal, C.K., Freeman, B.D., Rautenbach, R., Corrections for analytical gas-permeation models for separation of binary gas mixtures using membrane modules, Journal of Membrane Science, **118,** 289-294 (1996).
13. Babaluo, A.A. and Razmjoo, A., Manufacturing of alumina-ceria nanocomposite membranes for removing of volatile organic compounds, ANVOC Symposium, Istanbul, Turkey, 29-36 (30 – 31 May, 1 June 2005).
14. Sridhar, S. and Khan, A. A., Simulation studies for the separation of propylene and propane by ethyl-cellulose membrane, Journal of Membrane Science, **159,** 209-219 (1999).
15. Pan, C.Y. and Habgood, H.W., An analysis *of* the single-stage gaseous permeation process, Ind. Eng. Chem. Fundam., **13,** 323 (1974).
16. Conesa, A., Roura, F., Pitarch, J.A., Vicente-Mingarro, I., Rodriguez, M.A., Separation of binary gas mixtures by means of sol gel modified ceramic membranes. Prediction of membrane performance, Journal of Membrane Science, **155,** 123-131, (1999).
17. Giglia, S., Bikson, B., Perrin, J. E., Donatelli, A. A., Mathematical and experimental analyses of gas separation by hollow fiber membranes, Ind. Eng. Chem. Res. **30,** 1239 (1991).

18. Kaldis, S.P., Kapantaidakis, G.C., Papadopoulos, T.I. and Sakellaropoulos, G. P., Simulation of binary gas separation in a hollow fiber asymmetric membrane by orthogonal collocation, Journal of Membrane Science, **142,** 43-59 (1998).

Appendix A

Development of eqns (18)-(20)

From the eq.5 of the text:

$$\frac{dx}{dR^f} = \frac{(x-y)\{\alpha(1-x)(x-\gamma y) - x[1-x-\gamma(1-y)]\}}{(y-x_f)} \tag{5}$$

By substituting for y from eq.(16) in eq.(5),one have:

$$\frac{dx}{dR^f} = \{\alpha(1-x_f)(x_f-\gamma x_f) - x_f[1-x_f-\gamma(1-x_f)]\} \tag{A1}$$

After simplification:

$$\frac{dx}{dR^f} = -(1-x_f)x_f(1-\gamma)R_f(\alpha-1) \tag{A2}$$

Eq.A2 is integrated from x_f to x and $R^f=0$ to R^f to obtain:

$$x = x_f + -(1-x_f)x_f(1-\gamma)R_f(\alpha-1) \tag{A3}$$

or

$$x = x_0 + x_1(\alpha-1) \tag{18}$$

where $x_0 = x_f$ and the first order solution is $x_1 = -(1-x_f)x_f(1-\gamma)R_f$.

Eq 19 can be obtained by a similar way from the eq.6 of the text.

From the eq.4 of the text:

$$-\frac{d(L^*)}{d(R^f)} = \frac{d(V^*)}{d(R^f)} = \alpha(x-\gamma y) + [(1-x)-\gamma(1-y)] \tag{4}$$

By substituting for y from eq.(16) in eq.(4), one have:

$$-\frac{d(L^*)}{d(R^f)} = \alpha(x_f-\gamma x_f) + [(1-x_f)-\gamma(1-x_f)] \tag{A4}$$

After the simplification:

$$-\frac{d(L^*)}{d(R^f)} = (1-\gamma)[\alpha.x_f + (1-x_f)] \tag{A5}$$

Eq.A4 is integrated from $L^*=1$ to L and $R^f=0$ to R^f to obtain:

$$L^* = 1 + (\gamma-1)R^f - x_f(\gamma-1)R^f(\alpha-1) \tag{A6}$$

or

$$L^* = L_0^* + L_1^*(\alpha-1) \tag{20}$$

where $L_0^* = 1 + (\gamma-1)R^f$ and the first order solution is $L_1^* = -x_f(\gamma-1)R^f$.